



NLR-TP-98343

**Analysis of the data from a distributed set of  
accelerometers, for reconstruction of set  
geometry and its rigid body motion**

J.P.B. Vreeburg



NLR-TP-98343

## **Analysis of the data from a distributed set of accelerometers, for reconstruction of set geometry and its rigid body motion**

J.P.B. Vreeburg

This investigation has been carried out under a contract awarded by the Netherlands Agency for Aerospace Programmes (NIVR), contract number 02601N. NIVR has granted NLR permission to publish this report.

This report is based on a presentation held at the Space Technology and Applications International Forum (STAIF-99), Conference on International Space Station Utilization, January 31 - February 4, 1999, Albuquerque, New Mexico, U.S.A.

The contents of this report may be cited on condition that full credit is given to NLR and the author.

Division:	Space
Issued:	August 1999
Classification of title:	unclassified



**Contents**

<b>INTRODUCTION</b>	3
<b>THE OUTPUT FROM AN ACCELEROMETER ON A MOVING FRAME</b>	5
<b>RECONSTRUCTION OF ACCELEROMETER GEOMETRIC ERRORS</b>	6
<b>RECIPE FOR AN ITERATED SOLUTION</b>	8
<b>EXAMPLES</b>	9
<b>RECONSTRUCTION OF MOTION VECTORS</b>	11
<b>PLANAR DECOMPOSITION OF A QUADRATIC FORM</b>	12
<b>RECONSTRUCTION OF <math>\Omega</math></b>	13
<b>DISCUSSION</b>	14
<b>SPECIAL ARRANGEMENTS</b>	14
<b>CONCLUSIONS</b>	16
<b>REFERENCES</b>	16

3 Figures

(18 pages in total)



# ANALYSIS OF THE DATA FROM A DISTRIBUTED SET OF ACCELEROMETERS, FOR RECONSTRUCTION OF SET GEOMETRY AND ITS RIGID BODY MOTION

J.P.B. Vreeburg

*National Aerospace Laboratory NLR, P.O. Box 90502, 1006 BM Amsterdam, The Netherlands  
email: vreeburg@nlr.nl*

**Abstract.** The paper reports on a current line of research in accelerometry. Two subjects are addressed: the reconstruction of the location and attitude of a linear, or uni-axial, accelerometer from its output under a known motion, and the reconstruction of the acceleration field constituent vectors from the combined output of a known arrangement of linear accelerometers.

The arrangement can be arbitrary and, consequently, does not require precision mounting.

The component of the acceleration along the sensitive direction gives the ideal output of the accelerometer. When the motion that induces the acceleration is known, a set of five ideal measurement data may suffice to recover the location and attitude of the accelerometer. The formulae for this calculation are given. Their use is illustrated by simulation of an accelerometer and its output. The effects of errors are shown; it is found that noisy data are much less detrimental to the reconstruction calculations than systematic errors in the known motion.

If the geometry of a set of accelerometers is known, their output can be combined for the reconstruction of the linear and angular motion components that induce the acceleration. Conventionally this is achieved by elimination of the contribution of the angular rate of the geometry to the acceleration field. Only special arrangements of accelerometers, discussed in the literature, allow elimination by elementary operations.

A method, thought to be new, is presented for the elimination of the linear and angular acceleration contributions to the field sensed by an arbitrary arrangement of accelerometers, and the consequent recovery of the angular rate vector from the reduced data set. Particular difficulties are encountered in this process but it has been shown that successful reconstruction is possible when a redundant set of data is available.

Various options are suggested for further analysis, with the goal to determine the minimum arrangement, identify system errors or improve data accuracy.

## INTRODUCTION

The motion of a rigid frame induces an acceleration field on the frame, except for the trivial case of uniform translation in inertial space. Many authors have reported on their schemes to recover the motion from measurements of the field strength at discrete locations on the frame. In practice, the frame is a rigid structure that supports a precisely engineered arrangement of linear accelerometers; 9 is a common number. A well-known publication on the subject is (Padgaonkar, 1979), but many earlier and later papers have appeared.

An alternative method to determine the motion is to measure with gyroscopes the rate of rotation of the frame, and the linear acceleration at the origin with a tri-axial accelerometer. The angular acceleration could then be determined by numerical differentiation of the angular rate. Such an instrument is an 'inertial platform', and highly accurate ones exist. Accuracy comes at a price and the all-accelerometer device has a cost advantage when its performance is acceptable. Other generic advantages of the accelerometers are their robustness, low mass and low power requirements. Quite accurate devices are made in silicon, integrated with their electronics on a chip.

There are applications in which the accuracy advantages of the inertial platform cannot be realized. In general this occurs if the motion has components with prominent peaks, as when the frame is moved by a blast (Bulmash, 1989). Thus, the all-accelerometer device is used commonly to determine the motion of dummy body parts during car crash investigations (Padgaonkar, 1979; Plank, 1989). If the accuracy is not needed for the integration of motion, then the requirements become less stringent and the accelerometers are preferred again, for example in gait studies (Hayes, 1983; Ladin, 1991). The low costs of implementation make the functionality attractive to system designers in various fields (Chen, 1994; Frere, 1991) but no wide-spread use is observed.

The reason could be the disadvantages of an accelerometer arrangement. Although the data from six sensors should suffice to reconstruct the motion, the processing of the data usually requires integration of a system of coupled nonlinear equations, and this system may not be stable. So, the number of sensors is increased to nine, with a corresponding increase in costs. Pre-processing of the sensor data involves the elimination of the linear acceleration components from the data, and, commonly, of the angular rate components also. The elimination is achieved arithmetically and is feasible only for special, very regular geometries. As a consequence, it becomes expensive to construct an arrangement that can be analysed, and error analysis is very complicated (Plank, 1989).

The contribution of the present paper is in two areas. First will be given an analysis that shows for a single accelerometer the determination of its seismic point location and the direction of its sensitive axis. The analysis is similar to that in (Chen, 1994) but is formulated differently. Second will be presented the algebraic solution of the linear and angular acceleration vectors and of the angular rate vector, from the output of an arbitrary arrangement of nine accelerometers. This solution is original and may thus be new. The advantage of the solution would be that no costly precision mounting of accelerometers is necessary, and that the solution is not subject to divergence from accumulated integration errors. Evidently, there is redundancy since the angular rate is the integrated value of the angular acceleration. The redundancy can be exploited in various ways, to reduce the number of sensors (and incur integration) or to determine error magnitudes (including bias and scale-factor errors). In this paper no attention is given to these matters.

The impetus for the study has been the incorporation of an arrangement of nine linear accelerometers in a special configuration as the main instrument of the Ejectable Ballistometer, the test article of the Wet Satellite Model experiment (Vreeburg, 1994a). In this experiment, launched by sounding rocket, has been determined the effect of liquid in a partially filled tank on the motion of a spinning spacecraft. Presently, a distributed arrangement of six accelerometers, together with three gyroscopes, makes up the motion sensing system of the Sloshsat FLEVO<sup>1)</sup> spacecraft (Dujardin, 1997).

---

<sup>1)</sup> Sloshsat FLEVO is a harmonized programme between the European Space Agency (ESA) and the Netherlands Agency for Aerospace Programs (NIVR). Main contractor is the National Aerospace Laboratory NLR (The Netherlands) with participation of Fokker Space (The Netherlands), Verhaert (Belgium), Newtec (Belgium), Rafael (Israel) and NASA (USA). The Sloshsat FLEVO development is performed in the framework of the ESA Technology Development Programme (TDP) Phase 2 and the NIVR Research and Technology (NRT) programme.



## THE OUTPUT FROM AN ACCELEROMETER ON A MOVING FRAME

In the moving frame the location of the seismic point of the accelerometer is represented by vector  $\underline{\mathbf{R}}$ . The sensitive direction is given by unit vector  $\underline{\mathbf{s}}$ . All vectors will be taken as column vectors. The field at location  $\underline{\mathbf{R}}$  is given by (Goldstein, 1980):

$$\underline{\sigma}(\underline{\mathbf{R}}) = \underline{\sigma}_L + (\{\dot{\underline{\Omega}}\} + \{\underline{\Omega}\}^2) \underline{\mathbf{R}}. \quad (1)$$

The acceleration at the origin of the frame is obtained from  $\underline{\mathbf{R}} = 0$ .

The frame rotation rate is  $\underline{\Omega}$ , its angular acceleration rate is  $\dot{\underline{\Omega}}$ . A skew-symmetric matrix formed from a vector to effect the cross-product is represented by putting the vector in curly brackets, { }.

The output from an ideal (no bias or scalefactor errors) accelerometer with sensitive axis direction  $\underline{\mathbf{s}}$  is:

$$\mathbf{p} = \underline{\mathbf{s}} \cdot [\underline{\sigma}_L + (\{\dot{\underline{\Omega}}\} + \{\underline{\Omega}\}^2) \underline{\mathbf{R}}]. \quad (2)$$

The scalar product of two vectors  $\underline{\mathbf{a}}$  and  $\underline{\mathbf{b}}$  is written as  $\underline{\mathbf{a}} \cdot \underline{\mathbf{b}}$ .

For simulation of motion a Matlab program has been written. It allows specification of each of the three components of linear acceleration and each of the three components of angular acceleration. Each of the six entries consists of eight numbers, as follows:

a d s a1 f1 a2 f2 ns

- a = amplitude of block function
- d = length of block
- s = waiting interval before the sinusoidal functions start
- a1 = amplitude of function  $\sin(2\pi f1 t)$
- a2 = amplitude of function  $\sin(2\pi f2 t)$
- ns = noise amplitude.

The motion is generated for an equispaced sequence of N instances. At each instance the value of an acceleration component is obtained by addition of the instantaneous values of the block function, the sinusoidal functions and a random number between -1 and +1, multiplied by ns.

The block function starts with a zero amplitude for d instances, then d instances of amplitude a, followed by 2d instances with zero amplitude and again d with amplitude -a, followed by 2d with zero amplitude. Thus, from the start of nonzero amplitude, a period of 6d has been covered. A similar period, but now with d increased to 2d, is entered and once again with a 3d interval. From the start altogether 37d instances have been consumed. A next period of 37d instances is entered, but now with the amplitude increased to 2a. Next, the amplitude is increased to 3a and so on, until the N instances run out. When the motion is given by the block function only, noise is not added to the components with zero amplitude.

The rotational acceleration is integrated to yield the instant values of the angular rate in the sequence. Extra noise is not added.

The motion specification allows for uniform motions, impulsive changes, and may include low and high frequency components.

When a seismic point location vector  $\underline{R}$  and a sensitive axis direction  $\underline{s}$  is specified, substitution in equation (2) will yield a sequence of N equispaced sensor output data  $p(i)$ ,  $i=1,2,\dots,N$ .

### RECONSTRUCTION OF ACCELEROMETER GEOMETRIC ERRORS

Considered will be the determination of the actual location of the seismic point  $\underline{R}_o$ , and the actual sensitive axis direction  $\underline{s}_o$  of an ideal accelerometer, from the output of the accelerometer and known approximate values of  $\underline{R}_o$  and  $\underline{s}_o$ . The analysis is restricted to the case that  $\underline{R}$  and  $\underline{s}$  are not parallel. This represents a simplified configuration that can be dealt with differently.

Form unit vector  $\underline{r}$  from  $\underline{R} = R \underline{r}$ , and unit vector  $\underline{t}$  from  $\sin\phi \underline{t} = \{s\} \underline{r}$ .  
Then,

$$\underline{r} = \cos\phi \underline{s} - \sin\phi \{s\} \underline{t}. \quad (3)$$

Note that for small  $\phi$ ,  $\underline{t}$  can be much in error.

From the orthogonal triad  $\underline{r}$ ,  $\underline{t}$ ,  $\{s\} \underline{t}$ , form orthogonal matrix  $[Q]$ .

$$[Q] = [\underline{s} \underline{t} \{s\} \underline{t}]. \quad (4)$$

The same construction performed with the true values of  $\underline{R}$  and  $\underline{s}$  provides  $[Q_o] = [\underline{s}_o \underline{t}_o \{s_o\} \underline{t}_o]$ .

Define an orthogonal matrix  $[U] = [\underline{u}_1 \underline{u}_2 \underline{u}_3] = [Q]^T [Q_o]$ , where a superscript T denotes transpose.

A vector  $\underline{V}_o$  has components  $\underline{V}$  along the unit vectors that form  $[Q]$ ; a similar relation holds for  $[Q_o]$ , and so one finds:

$$\underline{s}_o \cdot \underline{V}_o = \underline{u}_1 \cdot \underline{V}; \quad \underline{t}_o \cdot \underline{V}_o = \underline{u}_2 \cdot \underline{V}; \quad \underline{V}_o \cdot \{s_o\} \underline{t}_o = \underline{u}_3 \cdot \underline{V}. \quad (5)$$

The known true motion of the frame that holds the accelerometer is:  $\underline{\sigma}_o$ ,  $\underline{\Omega}_o$ , and  $\dot{\underline{\Omega}}_o$ . In frame  $[Q]$  the motion is given by the same vectors without subscript.

The output of the accelerometer is obtained by substitution of the motion and the actual vectors  $\underline{R}_o$  and  $\underline{s}_o$  in equation (2), and yields:

$$p_o = \underline{s}_o \cdot \underline{\sigma}_o = \underline{s}_o \cdot \underline{\sigma}_L + R_o \left[ -\sin\phi_o \underline{t}_o \cdot \dot{\underline{\Omega}}_o + \left( \underline{s}_o \cdot \underline{\Omega}_o \right) \left( \underline{r}_o \cdot \underline{\Omega}_o \right) - \Omega_o^2 \underline{r}_o \cdot \underline{s}_o \right] \quad (6)$$

where  $\Omega_o^2 = \underline{\Omega}_o \cdot \underline{\Omega}_o = \Omega_o'^2$ .

Substitution of the vector products with the expressions from equation (5) gives:

$$p_o = \underline{u}_1 \cdot \underline{\sigma}_L + R_o \left[ -\sin\phi_o \underline{u}_2 \cdot \dot{\underline{\Omega}}_o + \underline{u}_1 \cdot \underline{\Omega}_o \left( \cos\phi_o \underline{u}_1 \cdot \underline{\Omega}_o - \sin\phi_o \underline{u}_3 \cdot \underline{\Omega}_o \right) - \cos\phi_o \Omega_o^2 \right]. \quad (7)$$

If [Q] is close to [Q<sub>o</sub>], [U] is close to the identity matrix [1], and can be written

$$[U] \sim [1] - \{\varepsilon\}, \text{ where } \underline{\varepsilon}^T = [\varepsilon_1 \ \varepsilon_2 \ \varepsilon_3] \text{ and } \underline{\varepsilon} \cdot \underline{\varepsilon} \ll 1. \quad (8)$$

For later reference it is convenient to write the expression that makes [U] exactly orthogonal for any value of  $\underline{\varepsilon}$ :

$$[U] = [1] - \{\varepsilon\} + 1/(1+\cos A) \{\varepsilon\}^2 \quad \text{where } A = \arcsin(\sqrt{\underline{\varepsilon} \cdot \underline{\varepsilon}})$$

From equation (8) follows:

$$\underline{u}_1^T = [1 \ -\varepsilon_3 \ \varepsilon_2]; \quad \underline{u}_2^T = [\varepsilon_3 \ 1 \ -\varepsilon_1]; \quad \underline{u}_3^T = [-\varepsilon_2 \ \varepsilon_1 \ 1]. \quad (9)$$

Substitution of the relations (9) in equation (7) and neglect of terms of second order small, yields:

$$\begin{aligned} p_o = \sigma_{L_1} - R_o \left[ \sin\varphi_o (\dot{\Omega}_2 + \Omega_1 \Omega_3) + \cos\varphi_o (\Omega_2^2 + \Omega_3^2) \right] + \\ \left[ \varepsilon_1 \ \varepsilon_2 \ \varepsilon_3 \right] \cdot \begin{bmatrix} R_o \sin\varphi_o (\dot{\Omega}_3 - \Omega_1 \Omega_2) \\ \sigma_{L_3} + R_o [2 \cos\varphi_o \Omega_1 \Omega_3 - \sin\varphi_o (\Omega_3^2 - \Omega_1^2)] \\ -\sigma_{L_2} - R_o [2 \cos\varphi_o \Omega_1 \Omega_2 + \sin\varphi_o (\dot{\Omega}_1 - \Omega_2 \Omega_3)] \end{bmatrix}. \end{aligned} \quad (10)$$

where a vector  $\underline{V}$  has component  $V_1$  along  $\underline{s}$ ,  $V_2$  along  $\underline{t}$ , etc.

A special case occurs if  $\underline{\sigma}_1 = 0$  and  $\dot{\underline{\Omega}} = 0$ . Denote the output by  $\pi_i$  if it is the result of a motion  $\Omega_i$ . Substitution in equation (10) gives:

$$\pi_1 = \varepsilon_2 R_o \sin\varphi_o \Omega_1^2; \quad \pi_2 = -R_o \cos\varphi_o \Omega_2^2; \quad \pi_3 = -R_o (\cos\varphi_o + \varepsilon_2 \sin\varphi_o) \Omega_3^2 \quad (11)$$

or:

$$R_o \cos\varphi_o = -\frac{\pi_2}{\Omega_2^2} = -\left( \frac{\pi_3}{\Omega_3^2} + \frac{\pi_1}{\Omega_1^2} \right); \quad \varepsilon_2 R_o \sin\varphi_o = \frac{\pi_1}{\Omega_1^2} = \frac{\pi_2}{\Omega_2^2} - \frac{\pi_3}{\Omega_3^2}. \quad (12)$$

Hence  $-2 R_o \cos\varphi_o = \frac{\pi_1}{\Omega_1^2} + \frac{\pi_2}{\Omega_2^2} + \frac{\pi_3}{\Omega_3^2}$  for any system [Q].

Thus, if one could induce uniform rotations about the principal axes of an invariable solid carrier of the accelerometer, the resulting output may be combined to yield  $R_o \cos\varphi_o$ .

Introduce the small difference between the actual values  $R_o$  and  $\varphi_o$ , and the known values  $R$  and  $\varphi$ :

$$R_o = R + \delta; \quad \varphi_o = \varphi + \theta; \quad \cos\varphi_o \sim \cos\varphi - \theta\sin\varphi; \quad \sin\varphi_o \sim \sin\varphi + \theta\cos\varphi$$

in order to obtain the error equation with five unknown error variables

$$p_o - p = [\delta \quad \theta \quad \varepsilon_1 \quad \varepsilon_2 \quad \varepsilon_3] \cdot \begin{bmatrix} -\sin\varphi(\dot{\Omega}_2 + \Omega_1\Omega_3) - \cos\varphi(\Omega_2^2 + \Omega_3^2) \\ R[-\cos\varphi(\dot{\Omega}_2 + \Omega_1\Omega_3) + \sin\varphi(\Omega_2^2 + \Omega_3^2)] \\ R\sin\varphi(\dot{\Omega}_3 - \Omega_1\Omega_2) \\ \sigma_{L_3} + R[2\cos\varphi\Omega_1\Omega_3 - \sin\varphi(\Omega_3^2 - \Omega_1^2)] \\ -\sigma_{L_2} - R[\sin\varphi(\dot{\Omega}_1 - \Omega_2\Omega_3) + 2\cos\varphi\Omega_1\Omega_2] \end{bmatrix}. \quad (13)$$

The term  $p$  is the predicted value of the measurement, calculated with the known values of the accelerometer geometry variables, i.e. the value  $p_o$  would have in absence of errors.

### RECIPE FOR AN ITERATED SOLUTION

In order to identify the location and sensitive axis direction of a linear accelerometer one needs to have approximate values of these parameters. They are used to calculate initial values of  $R$ ,  $\varphi$ , and  $[Q]$ , see equations (3) and (4).

Available are a number of accelerometer output data, duly corrected for instrument errors, and the values of motion vectors  $\underline{\sigma}_i$ ,  $\underline{\Omega}$ , and  $\dot{\underline{\Omega}}$  at the times of the data. The motion vectors are used to construct the predicted outcomes of the measurements, according to equation (6) without subscript  $o$ , and the column vector in equation (13). Thus a system of equations (13) is obtained. The number of equations needs to be larger than four, for batch processing.

The least-squares solution of system (13) yields values for  $\delta$ ,  $\theta$ , and  $\underline{\varepsilon}$ . These are used to update the values of the known parameters, with:

$$R_{new} = R_{old} + \delta; \quad \varphi_{new} = \varphi_{old} + \theta; \quad [Q]_{new} = [Q]_{old} * [U]$$

where  $[U]$  is constructed from  $\underline{\varepsilon}$ , by the formula that makes  $[U]$  exactly orthogonal, see below equation (8). This needs to be done because otherwise the relatively large errors early in the iteration get incorporated in  $[Q]$  and inhibit iteration at small errors.

Trial of the procedure with 5 data showed convergence to within machine accuracy with about 4 iterations, depending on the condition number of the coefficient matrix and the size of the initial error. Evidently, the direct iteration method need not be used to get the solution, many alternative methods are available.



### EXAMPLES

The reconstruction of the accelerometer geometry is attempted for true conditions:

$$R_o = 0.3 \text{ m}; \quad \underline{r}_o^T = [1 \ 0 \ 0]; \quad \underline{s}_o^T = [0 \ 1 \ 0].$$

The known geometry is put at:

$$R = 0.3111 \text{ m}; \quad \underline{r}^T = [0.9985 \ 0.0272 \ 0.0470]; \quad \underline{s}^T = [-.1766 \ 0.9810 \ 0.0801]$$

$$\text{thence: } \underline{R}^T - \underline{R}_o^T = [0.0107 \ 0.0085 \ 0.0146] \text{ m.}$$

The motion parameters are, in  $\text{m.s}^{-2}$  for linear acceleration, in  $\text{s}^{-2}$  for angular acceleration (see entry definitions under equation (2)):

$$\text{coefficient array} = \begin{bmatrix} 1 & 3 & 0 & 0.5 & 0.03 & 0.1 & 0.02 & 0 \\ 0.5 & 1 & 5 & 0.5 & 0.04 & 0.2 & 0.03 & 0 \\ 0.5 & 1 & 10 & 0.3 & 0.03 & 0.2 & 0.01 & 0 \\ 0 & 0 & 20 & 2 & 0.05 & 0.1 & 0.02 & 0 \\ 0 & 0 & 30 & 1 & 0.05 & 0.3 & 0.01 & 0 \\ 0.1 & 2 & 30 & 1 & 0.05 & 0.3 & 0.33 & 0 \end{bmatrix}.$$

The output of the accelerometer due to the motion specified by the array is plotted in figure 1 for 100 instances.

#### Case 1:

The nonzero amplitudes in column 1 of the array are disturbed with a random number between -0.01 and +0.01 at each instance. The amplitude of the periodic function that is obtained by adding the contributions of the low and high frequency component is at each instance disturbed also by a random number between -0.01 and +0.01. The disturbed motion is used to predict the outcome of the measurement of an ideal accelerometer with the known geometry. The difference between the true and the predicted measurements is plotted in figure 2.

When the solution for the true geometry is iterated with the first 30 data in the sequence the result is:

$$\underline{R}^T = [0.2903 \ 0.0012 \ -.0022] \text{ m} \quad \text{and} \quad \underline{s}^T = [0.0045 \ 1.0000 \ -.0030].$$

When only the last 30 data in the sequence are used:

$$\underline{R}^T = [0.3080 \ 0.0044 \ -.0036] \text{ m} \quad \text{and} \quad \underline{s}^T = [-.0038 \ 1.0000 \ 0.0034].$$

When all 100 data are used:

$$\underline{R}^T = [0.2877 \ -.0051 \ -.0017] \text{ m} \quad \text{and} \quad \underline{s}^T = [0.0001 \ 1.0000 \ -.0025].$$

The conclusion is that all processing schemes yield results of about equal accuracy. Not much improvement over the initial estimate is realized on the distance to the seismic point location; the estimate of the sensitive direction clearly improves with more data.



Case 2:

The various motion components are not disturbed, but the output of the sensor is changed by a random number between -0.25 and +0.25.

Iteration, using all 100 data, did not diverge but the calculated values did change strongly between different iterations and were of no use for the determination of the true value. When the noise level was decreased to between -0.01 and +0.01 a typical result was:

$$\underline{\mathbf{R}}^T = [0.2981 \ 0.0017 \ 0.0115] \text{ m and } \underline{\mathbf{s}}^T = [-.0022 \ 1.0000 \ 0.0030].$$

If 30 data only are used, the results are too variable and have no practical value. The next tests have been done with use of the full set of 100 data. Reducing the noise level by half, and after that once more by half gave no spectacular improvement. The plot of the difference between the true and the actual data showed a noise-like behaviour with uniform amplitude.

Case 3:

In order to investigate the effects of systematic errors, the frequencies were multiplied by a factor 1.02. No noise was introduced.

When the results are iterated with the first 30 data:

$$\underline{\mathbf{R}}^T = [0.3084 \ 0.0042 \ 0.0013] \text{ m and } \underline{\mathbf{s}}^T = [0.0041 \ 1.0000 \ -.0054].$$

When the last 30 data only were used:

$$\underline{\mathbf{R}}^T = [0.1849 \ 0.0163 \ -.2595] \text{ m and } \underline{\mathbf{s}}^T = [-.1362 \ 0.9855 \ 0.1013].$$

During the first 30 instances, the effect of the disturbed frequencies does not act on the two acceleration components that are to be affected most. The results with these data are fine. With the last 30 data a location for the seismic point is calculated that is completely wrong, but the sensitive direction is reasonably correct. The difference between the true and the predicted measurements grows to about 0.5 m.s<sup>-2</sup>.

Multiplication of the frequencies by a factor 1.01 and using all 100 data yields:

$$\underline{\mathbf{R}}^T = [0.2184 \ -.0131 \ -.0725] \text{ m and } \underline{\mathbf{s}}^T = [-.0173 \ 0.9985 \ 0.0518]$$

and the magnitude of the difference between the true and the predicted measurements is 0.3 m.s<sup>-2</sup>.

The conclusion from the examples is that noisy data may still allow a useful identification of the true geometry of the accelerometer, as long as the motion parameters do not have systematic errors. If the frequency of the motion has an uncertainty of 1 %, it cannot be used to predict the outcome of the measurement with useful accuracy. This last conclusion may have to be modified if more data are used, sufficient to cover a large number of periods in the oscillatory motion.

## RECONSTRUCTION OF MOTION VECTORS

The motion of the frame that carries the accelerometers is given by the three vectors  $\underline{\sigma}_L$ ,  $\underline{\Omega}$ , and  $\dot{\underline{\Omega}}$ . It will be shown how these vectors can be recovered by algebraic solution of nine equations that represent the output of nine ideal accelerometers with known location of seismic point and direction of sensitive axis.

The set of equations is:

$$p_j = \underline{s}_j \cdot [\underline{\sigma}_L + (\{\dot{\underline{\Omega}}\} + \{\underline{\Omega}\}^2) \underline{R}_j], \quad j = 1 \text{ to } 9 \quad (14)$$

for definiteness is assumed  $\underline{s}_j \cdot \underline{R}_j > 0$ .

Introduce  $\underline{c}_j = \{\underline{R}_j\} \underline{s}_j$ , and write:

$$p_j - \underline{\Omega} \cdot \{\underline{s}_j\} \{\underline{R}_j\} \underline{\Omega} = \underline{s}_j \cdot \underline{\sigma}_L + \underline{c}_j \cdot \dot{\underline{\Omega}} = \begin{bmatrix} \underline{s}_j^T & \underline{c}_j^T \end{bmatrix} \begin{bmatrix} \underline{\sigma}_L \\ \dot{\underline{\Omega}} \end{bmatrix} \quad (15)$$

By singular value decomposition the  $9 \times 6$  matrix  $[\underline{s}_j^T \ \underline{c}_j^T]$  is written as  $[\underline{s}_j^T \ \underline{c}_j^T] = [\underline{K}] [\underline{D}] [\underline{L}]^T$ , where  $[\underline{K}]$  and  $[\underline{L}]$  are orthogonal matrices, of dimension 9 and 6 respectively, and  $[\underline{D}]$  is a  $9 \times 6$  matrix with nonzero elements on its principal diagonal only.

Denote the  $i$ -th column of matrix  $[\underline{K}]$  by  $\underline{k}_i$ . Multiplication of equation (15) by  $\underline{k}_\ell^T$  yields a zero on the right hand side for  $i=7, 8, \text{ or } 9$ . The result is written as:

$$\underline{\Omega} \cdot [\underline{A}_\ell] \underline{\Omega} = P_\ell \quad \ell=1, 2, \text{ or } 3 \quad (16)$$

$$\text{where: } [\underline{A}_\ell] = \frac{1}{2} \sum_{j=1}^9 k_{6+\ell,j} (\{\underline{s}_j\} \{\underline{R}_j\} + \{\underline{R}_j\} \{\underline{s}_j\}) = [\underline{A}_\ell]^T$$

$$\text{and } P_\ell = \sum_{j=1}^9 k_{6+\ell,j} p_j.$$

Note that matrix  $[\underline{A}_\ell]$  is symmetric since the quadratic form on the left hand side of equation (16) removes skew-symmetric components.

For each value of  $\ell$ , equation (16) gives a quadratic form in  $\underline{\Omega}$ . If at least three are available, vector  $\underline{\Omega}$  can be reconstructed, but not always uniquely. The difficulties will be discussed in the sequel. After reconstruction  $\underline{\Omega}$  is substituted back in the set of equations and these are solved for  $\underline{\sigma}_L$  and  $\dot{\underline{\Omega}}$  by standard methodology.

### PLANAR DECOMPOSITION OF A QUADRATIC FORM

Consider a quadratic form in  $\underline{\Omega}$  of special type:

$$\begin{aligned} \underline{s} \cdot \{\underline{\Omega}\}^2 \underline{R} &= \frac{1}{2} \underline{\Omega} \cdot (\{\underline{R}\}\{\underline{s}\} + \{\underline{s}\}\{\underline{R}\}) \underline{\Omega} = \\ &= \frac{1}{2} \underline{\Omega} \cdot [\underline{Q}]^T \text{diag} (-2\underline{s} \cdot \underline{R}; \underline{sR} - \underline{s} \cdot \underline{R}; -\underline{sR} - \underline{s} \cdot \underline{R}) [\underline{Q}] \underline{\Omega}. \end{aligned} \quad (17)$$

where  $\underline{R}^2 = \underline{R} \cdot \underline{R}$ , etc., 'diag' indicates a diagonal matrix, and orthogonal matrix  $[\underline{Q}]$  is:

$$[\underline{Q}] = \frac{1}{\sqrt{2 \underline{sR} (\underline{s}^2 \underline{R}^2 - (\underline{s} \cdot \underline{R})^2)}} \begin{bmatrix} \sqrt{2 \underline{sR}} \underline{c}^T \\ \sqrt{\underline{sR} - \underline{s} \cdot \underline{R}} (\underline{s} \underline{R}^T + \underline{R} \underline{s}^T) \\ \sqrt{\underline{sR} + \underline{s} \cdot \underline{R}} (\underline{s} \underline{R}^T - \underline{R} \underline{s}^T) \end{bmatrix}. \quad (18)$$

where  $\underline{c} = \{\underline{R}\} \underline{s}$ , and so  $\{c\} = \{\underline{R}\} \{\underline{s}\} - \{\underline{s}\} \{\underline{R}\}$ . Special case  $\underline{c}=0$  is excluded here.

The eigenvalues  $\lambda_i$ ,  $i=1,2,3$ , of any symmetric matrix  $[\underline{A}]$  become  $\lambda_i + \gamma$  as the three eigenvalues of matrix  $[\underline{A}] + \gamma [1]$  where  $[1]$  is the unit matrix. Order  $\lambda_1 \leq \lambda_2 \leq \lambda_3$ , and take  $\gamma = \lambda_2 - \lambda_1 - \lambda_3$ . Then the eigenvalues of matrix  $[\underline{A}] + \gamma [1]$  have the properties of the eigenvalues in the decomposition in (17), viz. the intermediate eigenvalue is equal to half the trace. Consequently:

$$\underline{\Omega} \cdot [\underline{A}] \underline{\Omega} = \frac{1}{2} \underline{\Omega} \cdot (\{\underline{R}\}\{\underline{s}\} + \{\underline{s}\}\{\underline{R}\}) \underline{\Omega} - \gamma \underline{\Omega}^2 \quad (19)$$

Since vectors  $\underline{R}$  and  $\underline{s}$  define a plane, the decomposition in (19) will be indicated as the 'planar' decomposition of matrix  $[\underline{A}]$ . It is noted that the actual values of  $\underline{R}$  and  $\underline{s}$  are obtained from the comparison of the orthogonal matrix that results from the decomposition of matrix  $[\underline{A}] + \gamma [1]$ , with matrix  $[\underline{Q}]$  in (18).

Define an orthonormal triad  $\underline{u}_1$ ,  $\underline{u}_2$ , and  $\underline{u}_3$ , with  $\underline{u}_1$  and  $\underline{u}_2$  in the plane defined by  $\underline{R}$  and  $\underline{s}$ . Then write:

$$\underline{R} = R_1 \underline{u}_1 + R_2 \underline{u}_2; \quad \underline{s} = s_1 \underline{u}_1 + s_2 \underline{u}_2; \quad z_1 = \frac{R_1}{R_2}; \quad z_2 = \frac{s_1}{s_2}; \quad b = R_2 s_2 \quad \text{in order to derive:}$$

$$\begin{aligned} \underline{\Omega} \cdot (\{\underline{R}\}\{\underline{s}\} + \{\underline{s}\}\{\underline{R}\}) \underline{\Omega} &= 2b \left[ z_1 z_2 (\underline{u}_1 \cdot \underline{\Omega})^2 + (\underline{u}_2 \cdot \underline{\Omega})^2 + \right. \\ &\left. + (z_1 + z_2) (\underline{u}_1 \cdot \underline{\Omega}) (\underline{u}_2 \cdot \underline{\Omega}) - (1 + z_1 z_2) \underline{\Omega}^2 \right]. \end{aligned} \quad (20)$$

### RECONSTRUCTION OF $\underline{\Omega}$

Angular rate  $\underline{\Omega}$  is written as  $\underline{\Omega}\underline{\omega}$ , where  $\underline{\omega} \cdot \underline{\omega} = 1$ . The planar decomposition of matrix  $[A_1]$  from equations (16) according to (20) followed by division with  $\Omega^2$ , yields:

$$\frac{P_1 - \gamma\Omega^2}{b\Omega^2} + z_1 z_2 + 1 = z_1 z_2 X^2 + (z_1 + z_2) X (\underline{u}_2 \cdot \underline{\omega}) + (\underline{u}_2 \cdot \underline{\omega})^2 \quad (21)$$

where  $X = \underline{u}_1 \cdot \underline{\omega}$ .

Similarly, matrix  $[A_2]$  can be decomposed with use of the orthonormal triad  $\underline{v}_1$ ,  $\underline{u}_2$ , and  $\underline{v}_3$ , where  $\underline{v}_1$  and  $\underline{u}_2$  are in the plane defined by the vectors found from the planar decomposition of  $[A_1]$ . It is essential that the orthonormal triad includes  $\underline{u}_2$ , used in the decomposition of  $[A_1]$ . Consequently  $\underline{u}_2$  is along the intersection of the planes found for  $[A_1]$  and  $[A_2]$ . Then, if one defines  $Y = \underline{v}_1 \cdot \underline{\omega}$ , an equation like (21) is found that relates  $Y$  to  $\underline{u}_2 \cdot \underline{\omega}$ . Since the equation is quadratic explicit solutions are obtained:

$$X_{1,2} = \frac{1}{2z_1 z_2} \left[ - (z_1 + z_2)(\underline{u}_2 \cdot \underline{\omega}) \pm \sqrt{(z_1 - z_2)^2 (\underline{u}_2 \cdot \underline{\omega})^2 + 4z_1 z_2 \left( 1 + z_1 z_2 + \frac{P_1 - \gamma\Omega^2}{b\Omega^2} \right)} \right]$$

and a similar expression for  $Y_{1,2}$ .

$X$ ,  $Y$ , and  $\underline{u}_2 \cdot \underline{\omega}$  are components of unit vector  $\underline{\omega}$ :

$$\underline{\omega} = \xi(-Y\underline{u}_3 + X\underline{v}_3) + (\underline{u}_2 \cdot \underline{\omega}) \underline{u}_2 \quad (22)$$

where  $\frac{1}{\xi} \sqrt{\xi^2 - 1} = \underline{u}_3 \cdot \underline{v}_3 = \underline{u}_1 \cdot \underline{v}_1$ .

Squaring equation (22) gives a scalar equation for  $\underline{u}_2 \cdot \underline{\omega}$ , to be solved iteratively.

The above derivation shows that each pair of the three equations in (16) yields a component of  $\underline{\omega}$ , provided that the magnitude  $\Omega$  is given. With three equations one can form three components, and these may be used to construct  $\underline{\omega}$ .

Denote the calculated components by  $\underline{u}_2 \cdot \underline{\omega}$ ,  $\underline{v}_2 \cdot \underline{\omega}$ ,  $\underline{w}_2 \cdot \underline{\omega}$ . If  $\Omega$  had been specified correctly, the components must combine to a unit vector, in formula:

$$(\underline{u}_2 \cdot \underline{\omega}) \underline{u}_2 + (\underline{v}_2 \cdot \underline{\omega}) \underline{v}_2 + (\underline{w}_2 \cdot \underline{\omega}) \underline{w}_2 = \underline{\omega} \quad (23)$$

Squaring equation (23) gives a scalar equation for the magnitude of  $\underline{\omega}$  that forms the basis for an iteration on the magnitude  $\Omega$ .

Thus, the complete system that needs to be solved by iteration consists of four equations. Three obtained by squaring equations (22) plus one from squaring equation (23). Magnitude  $\Omega$  is the independent variable.

## DISCUSSION

The equations above have a number of  $\pm$  signs that need to be made specific. If one starts from a given initial condition  $\underline{\Omega}_0$ , all signs can be initialized correctly, and a sequence of measurements can be processed to find the sequence of angular rate  $\underline{\Omega}$ .

In (Vreeburg, 1994b) the process outlined above has been used to find  $\underline{\Omega}$ . However, the algorithm was based on the primitive variables  $\underline{R}$  and  $\underline{s}$  that result from the planar decomposition of  $[A_\ell]$  rather than using the triad  $\underline{u}_1, \underline{u}_2, \underline{u}_3$  as done here. The iterated solution correctly produced the sequential values of  $\underline{\Omega}$  for a test case that had been chosen without special considerations. However if the sequence encountered measurements that resulted in a near zero value of the discriminant in one of the quadratic equations (see the solution for X above), no foolproof recipe could be given for the determination of the sign when the discriminant gained magnitude again. This difficulty was circumvented successfully by adding two more measurements, i.e. in the set (16) the value of  $\ell$  was increased to 5. With 5 data sequences there are 10 options to construct 3 components of  $\underline{\Omega}$ , and by choosing each time the 3 components that involved the largest discriminant values, no sign selection problem materialized. In other words, the solution was re-initialized at each step in the sequence to ensure good behaviour.

Various options may exist that achieve a reliable solution of  $\underline{\Omega}$ , e.g. new measurement equations could be formed by linear combinations of the equations (16). Another option is to exploit the relation between the angular rate and the angular acceleration to determine the signs. Or, the correct signs might be predetermined via simulations for all values of  $\underline{\Omega}$  and stored in a look-up table.

## SPECIAL ARRANGEMENTS

Figure 3 gives the arrangement of accelerometers in the ballistometer of (Vreeburg, 1994a). Another configuration, known in the literature as the 3-2-2-2 system, can be obtained by moving accelerometers 7, 8, and 9 in figure 3 to the origin and align these along the coordinate axes. A possible advantage of the ballistometer arrangement over 3-2-2-2 is its planar distribution that allows to package the system in a flat case.

Accelerometer 1 in figure 3 has its seismic point at  $[0 \ Rb \ ab]$  and the locations of the other seismic points can be surmised from the figure. The sensitive directions are indicated as well. If equation (14) is specialized for each accelerometer in figure 3, a set of 9 equations results. By elementary operations these equations can be reduced to 3 equations that have components of the angular rate only:

$$\begin{aligned}
 \Omega_x^2 + \frac{1}{2} (\Omega_y + \Omega_z)^2 &= (\underline{r}_1 \times \underline{\Omega})^2 = (p_1 + p_3 - \sqrt{2} p_7) / (Rb - ab) \\
 \Omega_y^2 + \frac{1}{2} (\Omega_x + \Omega_z)^2 &= (\underline{r}_2 \times \underline{\Omega})^2 = (p_4 + p_6 - \sqrt{2} p_8) / (Rb - ab) \\
 \Omega_z^2 + \frac{1}{2} (\Omega_x + \Omega_y)^2 &= (\underline{r}_3 \times \underline{\Omega})^2 = (p_2 + p_5 - \sqrt{2} p_9) / (Rb - ab)
 \end{aligned}
 \tag{24}$$

$$\underline{r}_1^T = \frac{1}{2} \sqrt{2} [0 \ 1 \ -1]; \quad \underline{r}_2^T = \frac{1}{2} \sqrt{2} [-1 \ 0 \ 1]; \quad \underline{r}_3^T = \frac{1}{2} \sqrt{2} [1 \ -1 \ 0].$$

The quadratic forms in (24) are of the special type exhibited in (17) with the additional property  $\underline{r} = \underline{s}$ .



When the 9 equations are reduced according to the procedure that results in equations (16) it is found that the matrices  $[A_q]$  are all members of the group with property:

$$[A] = (a+b+c) [1] + \begin{bmatrix} a & c & b \\ c & b & a \\ b & a & c \end{bmatrix}. \quad (25)$$

here, and in the sequel,  $[A]$ ,  $a$ ,  $b$ , and  $c$  have not a special meaning as given in earlier defined uses. The nondiagonal component in (25) is a 'circulant matrix'.

The eigenvalues of  $[A]$  are:

$$\begin{aligned} \mu_1 &= 2(a+b+c) \\ \mu_2 &= a + b + c + \sqrt{a^2+b^2+c^2-(ab+ac+bc)} \\ \mu_3 &= a + b + c - \sqrt{a^2+b^2+c^2-(ab+ac+bc)} \end{aligned} \quad (26)$$

if  $\sqrt{a^2 + b^2 + c^2 - (ab+ac+bc)} \geq a + b + c$ , then  $\mu_1$  is the intermediate eigenvalue and equal to half the trace of  $[A]$ .

Equality requires  $ab + ac + bc = 0$  and makes matrix  $[A]$  singular, or, aligns  $\underline{R}$  with  $\underline{s}$ . Linear combinations of  $[A_q]$  can be made to get the desired direction of  $\underline{R}$ , and yield the combination of sensor output that directly gives  $|\{R\}\underline{\Omega}|$ .

When the 9 equations that correspond to arrangement 3-2-2-2 are reduced to equations (16) one obtains matrices  $[A_q]$  with zero values on the diagonal, i.e.

$$[A] = \begin{bmatrix} 0 & c & b \\ c & 0 & a \\ b & a & 0 \end{bmatrix} \text{ and this matrix is of special type only if } abc = 0, \text{ and then } [A] = -\{u\}^2.$$

It is noted that the eigenvector that corresponds to the zero eigenvalue of  $[A]$  with  $abc = 0$  is:

$$\frac{[a^2(b-c) \quad b^2(c-a) \quad c^2(a-b)]}{(ab+ac+bc) \sqrt{a^2+b^2+c^2}}.$$

The three realisations (for  $a$  or  $b$  or  $c = 0$ ) form a plane, as do the three vectors  $\underline{f}_i$  in (24).

## CONCLUSIONS

Basic analyses have been presented of problems related to the use of a distributed set of ideal linear accelerometers for the measurement of the motion of their carrier. An ideal accelerometer is specified by five variables, viz. three to locate its seismic point, and two to identify the direction of its sensitive axis.

If the variables of an accelerometer are known approximately the exact values can be determined when the accelerometer output for exactly known motions is available. Noisy motion data are useful also, provided that no systematic errors exist in the known motion.

The nine vector components of a general motion can be resolved from the algebraic solution of the output equations from nine accelerometers, arbitrarily distributed. The solution process is rife with special cases and bifurcation points that need to be clarified for a complete theory. To be elaborated also is the exploitation of the redundancy in the system, for the reduction of the number of sensors in the arrangement, for the identification of instrument errors, for the improvement of the motion data accuracy, or for a combination of these goals.

Special arrangements of accelerometers are attractive for the property that wanted data can be obtained directly from linear combinations of output, i.e. without iterative processing. However, error analysis is required to obviate precision mounting of such special configurations. The formulae presented for the general arrangement need to be specialized in order to yield explicit expressions for the error terms.

## REFERENCES

- Bulmash, G., Loucks, R., Muller, P., and Pearson, R., "Dynamics of the Nine Linear Accelerometer System for Measuring Blast Induced Target Displacements," in *Computers in Engineering 1989*, Vol. 1, ASME, New York, 1989, pp. 179-182.
- Chen, J.H., Lee, S.C., and DeBra, D.B., "Gyroscope Free Strapdown Inertial Measurement Unit by Six Linear Accelerometers," *Journal of Guidance, Control, and Dynamics*, **17**, 2, 286-290 (1994).
- Dujardin, P.G.J.P., "Sloshsat FLEVO Motion Sensing Subsystem," presented at the *International Workshop on Spacecraft Attitude and Orbit Control Systems, IFAC, ESA/Estec, Noordwijk, NL, 15-17 Sept. 1997*. Also NLR TP 97451 U.
- Frere, P.E.M., "Problems of Using Accelerometers to Measure Angular Rate in Automobiles", *Sensors and Actuators A*, 25-27, 821-824 (1991).
- Goldstein, H., *Classical Mechanics*, 2nd Edition, Addison Wesley, Reading, Mass., 1980, p. 176.
- Hayes, W.C., Gran J.D., Nagurka, M.L., Feldman, J.M., and Oatis, C., "Leg Motion Analysis During Gait by Multiaxial Accelerometry: Theoretical Foundations and Preliminary Validations," *Journal of Biomechanical Engineering*, Transactions of the American Society of Mechanical Engineers, **105**, 283-289 (1983).
- Ladin, Z., and Wu, G., "Combining Position and Acceleration Measurements for Joint Force Estimation," *Journal of Biomechanics*, **24**, 12, 1173-1187 (1991).
- Padgaonkar, A.J., Krieger, K.W., and King, A.I., "Measurement of Angular Acceleration of a Rigid Body Using Linear Accelerometers", *Journal of Applied Mechanics*, Transactions of the American Society of Mechanical Engineers, **46**, 925-930 (1979).
- Plank, G., Weinstock, H., and Coltman, M., "Methodology for the Calibration of the Data Acquisition with a Six-Degree-of-Freedom Acceleration Measurement Device," DOT-TSC-NHTSA-88-3, Department of Transportation, Washington D.C., 1989.
- Vreeburg, J.P.B., "The Wet Satellite Model experiment," *Summary Review of Sounding Rocket Experiments in Fluid Science and Material Sciences*, ESA SP-114, Vol. 4, Oct. 1994a, pp. 9-21.
- Vreeburg, J.P.B., "On transforming accelerometer data to angular rate", *NLR TP 94241 U*, 1994b.

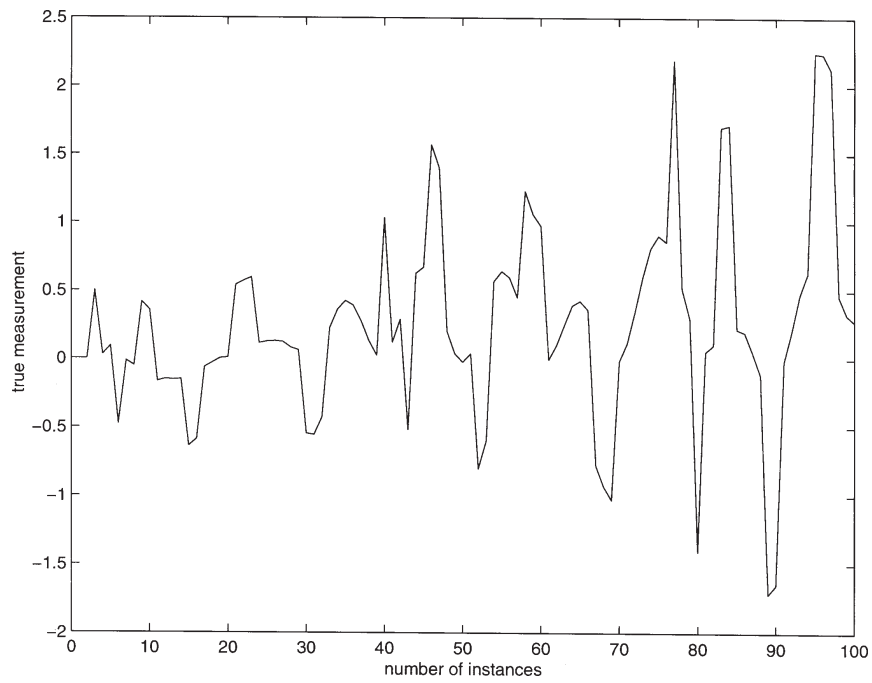


Fig.1 Simulated accelerometer signal

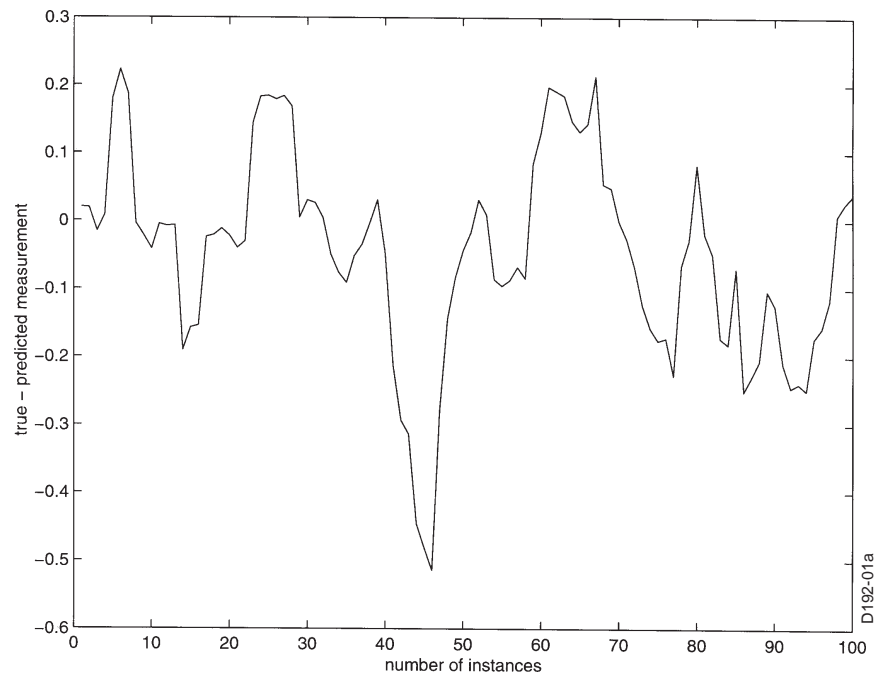


Fig.2 Difference between the exact and the predicted measurement

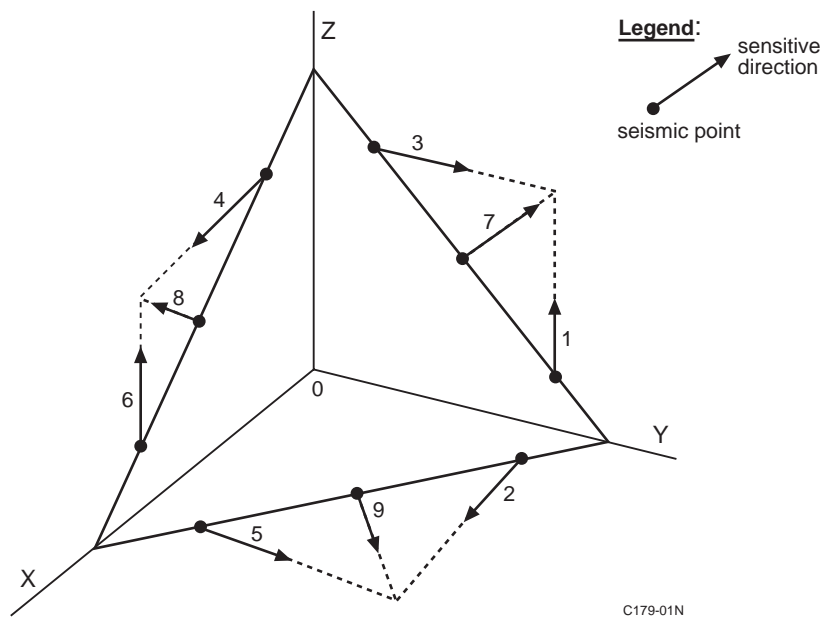
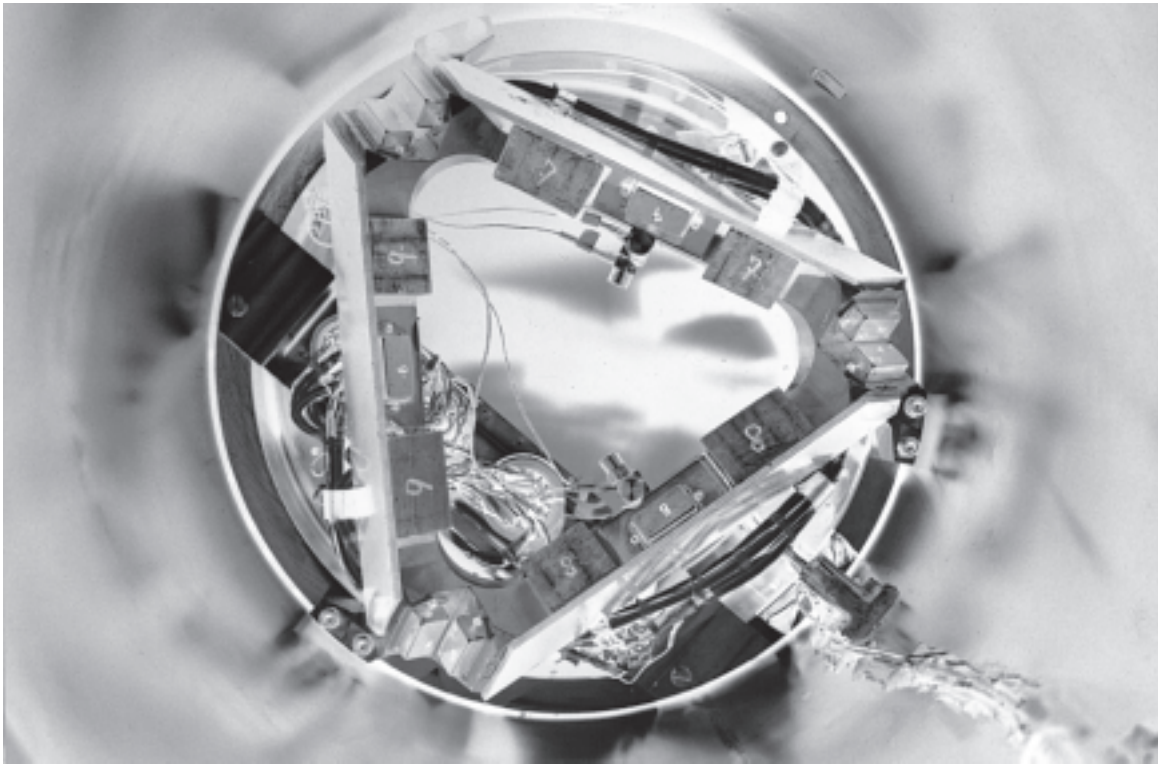


Fig.3 Configuration of the ballistometer